J Mater Sci: Mater Med (2009) 20:309–320
DOI 10.1007/s10856-008-3575-2

The fundamental parameters of chitosan in polymer scaffolds affecting osteoblasts (MC3T3-E1)

Wiroj Suphasiriroj · Pusadee Yotnuengnit · Rudee Surarit · Rath Pichyangkura

Received: 9 February 2008 / Accepted: 21 August 2008 / Published online: 13 September 2008

Abstract The aim of this study was to investigate the degree of deacetylation (DD) and molecular weight (MW) of chitosan within chitosan–collagen scaffolds on mouse osteoblasts (MC3T3-E1). The chitosan–collagen scaffolds were fabricated by freeze-drying technique. The studies on cell attachment and proliferation, alkaline phosphatase (ALP) activity, cell morphology, and mineralized nodule formation by osteoblasts on scaffolds were investigated. No statistically significant difference was found on cell attachment, but the chitosan–collagen scaffolds with low-DD chitosan had a statistically significantly ($P < 0.05$) higher proliferative effect and ALP activity than those scaffolds with high-DD chitosan, regardless of molecular weight. Scanning electron images demonstrated that MC3T3-E1 cells grew well on all test scaffolds; on the contrary, mineralized nodule formation was not found. In conclusion, the DD of chitosan is a crucial factor for MC3T3-E1 cells and it should be considered in further applications for bone tissue engineering.

W. Suphasiriroj (✉) · P. Yotnuengnit
Department of Oral Medicine, Faculty of Dentistry, Mahidol University, 6 Yothe Road, Rajthevee, Bangkok 10400, Thailand
e-mail: wiroj_bu@hotmail.com

R. Surarit
Department of Physiology and Biochemistry, Faculty of Dentistry, Mahidol University, Bangkok, Thailand

R. Pichyangkura
Department of Biochemistry, Faculty of Science, Chulalongkorn University, Bangkok, Thailand

1 Introduction

Bone regeneration is a critical issue in orthopedics, medicine, and dentistry. The recent progress in tissue engineering has opened the world of regeneration to a variety of organs and tissues, including bone. Three-dimensional porous scaffolds have been used extensively in bone tissue engineering for in vitro study of cell-scaffold interaction and in vivo study of tissue regeneration. These porous scaffolds serve as analogs of the extracellular matrix (ECM), acting both as physical support structures and as regulators of biological activity that affect cellular functions such as cell growth and differentiation. Several ECM-like materials that combine natural or synthetic polymers with collagen have been proposed for use as scaffolds [1–4]. Chitosan combined with collagen is one such material that offers various qualities advantageous for tissue generation [5–9].

Chitosan is a natural biopolymer that is a partially or completely deacetylated chitin and is composed of glucosamine and *N*-acetyl-glucosamine in a β (1–4) linkage. Chitosan is similar to glycosaminoglycans (GAGs) in structure and has numerous interesting physicochemical and biological properties. In acidic solution, the amine groups ($-NH_2$) of chitosan are protonated to $-NH_3^+$; the resulting cationic nature is primarily responsible for electrostatic interactions of chitosan with anionic GAGs, proteoglycans and other negatively charged molecules on the surface of cells [10, 11]. Depending on the source and preparation procedure, the molecular weight (MW) of chitosan can range from 50 to 2,000 kDa with the degree of deacetylation (DD) ranging from 40% to 98%. Fundamentally, all of the physicochemical properties of chitosan depend on these two fundamental parameters [10, 12]; these physicochemical properties include rheological

properties, antimicrobial activity, immunoadjuvant activity, enzyme-binding capacity, film and gel forming properties, mechanical properties, and membrane porosity [10, 12, 13]. Wang et al. suggested that the DD of chitosan had a great effect on its pKa, which increased from 6.17 to 6.51 as the DD decreased from 94.6% to 73.3%. The MW also influences the protonation constants pKas of chitosan, which were slightly decreased from 6.51 to 6.39 when the MW decreased from 1,370 to 60 kDa [14]. In addition, Chen et al. [15] reported that the MW of chitosan affected the thermal, mechanical, and permeability properties of chitosan membranes. Tensile strength, tensile elongation, and enthalpy of membranes prepared from high-MW chitosan were greater than those prepared from low-MW chitosan; on the other hand, membranes prepared from high-MW chitosan had lower permeability than those prepared from lower-MW chitosan.

Likewise, these fundamental parameters influence the biological properties of chitosan, including biocompatibility, cell attachment, cell proliferation, biodegradation by lysozyme, wound healing, and osteogenesis enhancement. Prasitsilp et al. [16] reported that the chitosan from shrimp and cuttlefish sources, which has a higher DD than other chitosans, supported the attachment of L929 fibroblasts and BHK21(C13) kidney cells, while chitosan with a lower DD did not. Howling et al. and Chatelet et al. [17, 18] suggested that a high-DD was more favorable for supporting L929 fibroblast cell growth, attachment and proliferation. Similarly, Mao et al. [19] demonstrated that chitosan membrane with a higher DD had stronger L929 fibroblast cell adhesion than did a membrane with a lower DD. Recently, Amaral et al. [20] reported that the attachment and proliferation of human osteoblastic MG-63 cells on chitosan films was dependent on the degree of acetylation (DA). For biodegradation, Varum et al. and Tomihata et al. [21, 22] suggested that highly deacetylated chitin showed slower biodegradation and evoked a milder tissue response than did less deacetylated chitin. Regarding osteogenic potential, Hidaka et al. [23] reported that membranes prepared with 65, 70, and 80% deacetylated chitin enhanced osteogenesis after implantation under rat calvarial periosteum; on the other hand, membranes prepared with 94% and 100% deacetylated chitin showed minimal osteogenesis.

Another versatile property of chitosan is that it can be molded into various forms including porous scaffolds in order to meet the demands of the different applications [24–26]. The properties of porous chitosan scaffolds, such as microstructure, crystallinity, and mechanical strength, can be varied by altering the concentration, MW and DD of the chitosan, including freezing rate [27, 28].

Several primary and transformed cell lines have been used to develop in vitro systems for studying interactions between cells and implant biomaterials. Immortalized cell lines are used often in these systems because they are relatively easy to maintain over a long period of time without loss of phenotypic expression as opposed to primary cell lines. A nontransformed MC3T3-E1 cell line derived from mouse calvaria has been used as a good in vitro model for studying interactions with implant biomaterials [29]. These cell lines (subclones 4 and 14) exhibit high levels of osteoblast differentiation after growth in ascorbic acid and inorganic phosphate and formed a well-mineralized ECM after 10 days in culture [30].

In general, osteoblastic cells arise from pluripotent mesenchymal progenitor cells and can then progress through the three developmental stages: proliferation, matrix maturation, and mineralization. Type I collagen and histone H4 expression in these cells peak during the proliferation phase, alkaline phosphatase (ALP) activity peaks during the matrix formation phase, while osteopontin and osteocalcin peak during the mineralization phase [31].

The aim of the this study was to investigate the effect of the DD and the MW of chitosan within chitosan–collagen scaffolds on osteoblasts (MC3T3-E1) including cell attachment and proliferation, ALP activity, cell morphology, and mineralized nodule formation.

2 Materials and methods

2.1 Preparation of chitosan and collagen solution

Chitosan, 80% deacetylated, was prepared by heterogeneous deacetylation of squid pen chitin, by soaking it in 50% (w/w) NaOH solution for 48–72 h or until 80% deacetylation was achieved [13, 32]. Partially *N*-acetyl chitosan, 50% deacetylated, was prepared by a homogenous deacetylation process. Chitin was solubilized in 40% NaOH (w/w) and the solution was allowed to deacetylate slowly at 4°C until the desired DD was achieved. The DD was determined by derivative UV spectroscopy [33].

Two preparations of 80% deacetylated chitosan and 50% deacetylated chitosan with low (160 kDa) and high (1,000 kDa) MW were used in this study. Low-MW, 80% deacetylated chitosan was prepared by enzymatic hydrolysis of chitosan using chitosanase produced from *Bacillus circulans* PP8, isolated from Phi Phi island, Thailand, while low-MW, 50% deacetylated was prepared by sonication of the 50% deacetylated solution using Dr. Hielscher GmbH sonicator (model UP400S, Stahnsdorf, Germany), Tip H7 sonotrode probe (1-cm diameter), at maximum power for 15 min. The low and high-MW of 80% deacetylated chitosan and 50% deacetylated were checked by gel permeation chromatography. Each chitosan solution (0.5% w/v) was made by solubilizing chitosans, according to their different DD and MW, in 1% acetic acid.

According to the procedure of O'Leary et al. [34] with slightly modification, type I collagen was extracted from rat-tail tendon by incubation in sterile 17 mM acetic acid with mechanical stirring for 48 h at 4°C. Undissolved tendon pieces were removed by centrifugation at 30,000 × *g* and 4°C (Beckman Model J2-21, Beckman Coulter, USA) for 60 min. The pH of the collagen solution was adjusted to 7.0 using sterile 0.1 M NaOH and the precipitated collagen was collected by centrifugation at 10,000 × *g* and 4°C (Hettich centrifuge, Tuttlingen, Andreas Hettich Gmbh&Co. KG, Germany) for 20 min. The collagen pellet was dissolved in sterile 17 mM acetic acid by stirring at 4°C for 48 h and then dialyzed through a molecular porous membrane (Spectra/Por® CE, MWCO:10,000, Spectrum Laboratories, Inc., USA) for 48 h. The pH of the collagen solution was adjusted to 7.0 with sterile 0.1 M NaOH and the precipitated collagen was collected by centrifugation at 10,000 × *g* and 4°C for 20 min. The resulting collagen pellet was frozen at −80°C prior to lyophilization for 48 h. Collagen solution (0.5% w/v) was made by solubilizing the collagen pellet in 1% acetic acid.

2.2 Scaffold preparation and characterization

To obtain a 0.25% chitosan–collagen solution, the equivalent volumes of the chitosan solution (0.50%) and the collagen solution (0.50%) were stirred together for 1 h. Subsequently, 100 µl of homogeneous chitosan–collagen solution was pipetted onto cover slips (12-mm diameter, 0.1-mm thick) and then frozen at −20°C for 24 hs. The samples were lyophilized under vacuum (<100 mTorr) at a condenser temperature of −40°C for 6 h to generate chitosan–collagen scaffolds. The chitosan–collagen scaffolds divided into four groups according to the DD and the MW of chitosan as follows:

Group 1: 80% DD and low-MW chitosan with collagen (80LMW-C);
Group 2: 80% DD and high-MW chitosan with collagen (80HMW-C);
Group 3: 50% DD and low-MW chitosan with collagen (50LMW-C);
Group 4: 50% DD and high-MW chitosan with collagen (50HMW-C);

These test scaffolds were compared with the controls: which were plain cover slips treated with 95% alcohol and 0.25% collagen scaffolds fabricated by the freeze-drying technique described above. For sterilization, the lyophilized test scaffolds and the controls were irradiated by under an ultraviolet lamp (30 W, 220 V) for 6 h.

The surface microstructures of the lyophilized test scaffolds were visualized by scanning electron microscopy (SEM; Hitachi S-2500, Hitachi Science System Ltd., Japan) at 300× magnification following sputter coating with platinum-palladium (Sputter coater, Hitachi E-120, Hitachi Science System Ltd., Japan). SEM images were scanned (Nikon Scantouch 210, Nikon Corporation, Taiwan) at 6.93% scale and 4,800 dpi resolution. Five fields were imaged per sample ($n = 5$). ImagePro Plus® Software Program Version 3.0 for Windows (Media Cybernectics, Gorgia, USA) was used to determine the surface pore size and the area fraction of the test scaffolds. Pore size was categorized into three pore diameter ranges: micropore (0–19 µm), medium-sized pore (20–50 µm), and macropore (51–100 µm; Fig. 1). Mean pore diameter in each pore was averaged by the lines that can be drawn to pass through the centroid position and join two points on each object's perimeter. The area fraction represented porosity and was calculated as follows:

$$\text{Area fraction}(\%) = \frac{\text{Area of bulk material}}{\text{Area of bulk material} + \text{Area of pore}} \times 100$$

2.3 Cell culture

MC3T3-E1 subclone 4 cells (ATCC number CRL-2593, Lot No. 3225550), derived from newborn mouse calvaria, were grown in alpha-Minimum Essential Medium (α-MEM, Gibco®, Invitrogen, California, USA) containing 10% fetal bovine serum (Hyclone®, Hyclone, Utha, USA), and antibiotic-antimycotic (10,000 unit/ml penicillin G, 10 mg/ml streptomycin, and 25 µg/ml amphoteracin B; Gibco®) and were incubated at 37°C in humidified air with 5% CO_2. The culture medium was changed every 2–3 days. MC3T3-E1 cells were subcultured after reaching confluence. The third to the fifth passages at 2×10^4 cells/well were used in these experiments. Cultures were characterized for cell attachment and proliferation, cell morphology, and functional activities (ALP activity and ability to form mineralized nodule).

2.4 Cell attachment and proliferation

The MTT assay (reduction of 3-(4,5-dimethylthiazol-2-yl)-2,5-diphenyltetrazolium bromide to a purple formazan product) was used to estimate cell attachment and cell proliferation as previously described [35]. MC3T3-E1 cells were plated at 2×10^4 cells/well on test scaffolds and controls in 24 well plates. At 5 and 24 h after cell attachment and on days 3, 5, 7, 10, and 14 of culture, cells were rinsed with phosphate buffer saline solution (PBS), and incubated with 500 µl/well of MTT (0.5 mg/ml; Sigma®, Sigma-Aldrich Pte Ltd., Singapore) for 2 h. This time period permitted the cellular conversion of MTT to

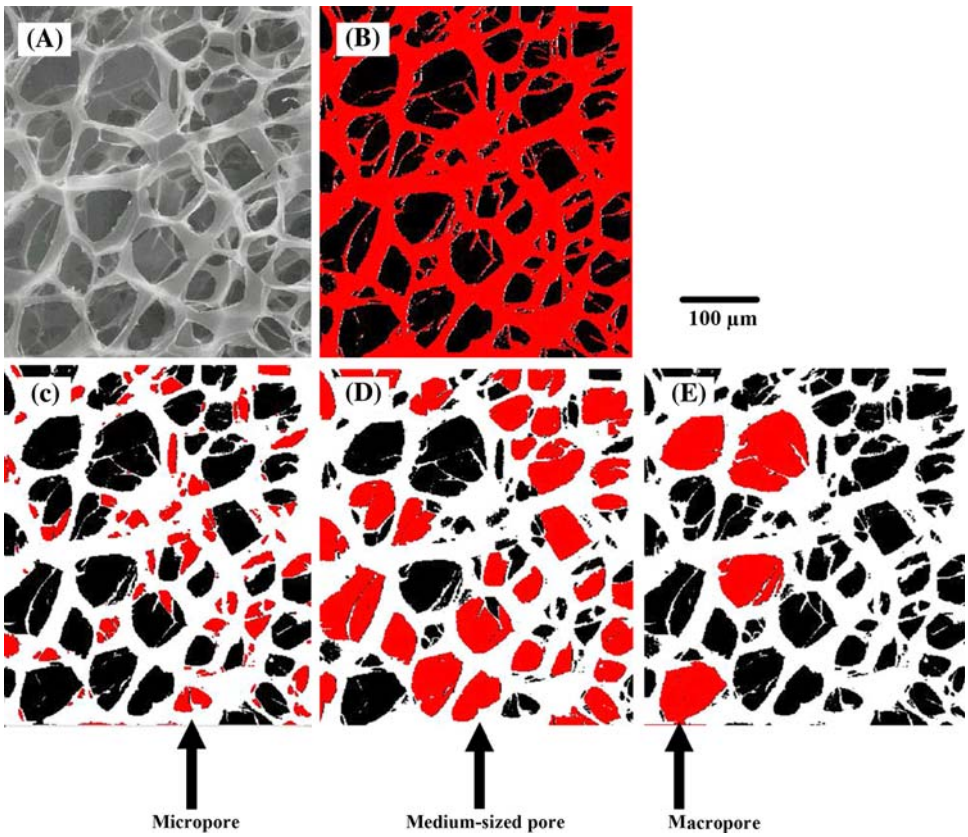

Fig. 1 Scanning electron microscopy image analysis by ImagePro® Plus Software Program; (**a**) original scaffolds, (**b**) area of bulk material (red area), (**c**) micropore (0–19 μm), (**d**) medium-sized pore (20–50 μm), (**e**) macropore (51–100 μm)

insoluble formazan salts, which were dissolved in 500 μl/well of dimethylsulfoxide (Sigma®). Absorbance was measured at 540 nm using an ELISA reader (Ceres 900, Biotech, USA). The optical densities (ODs) were calculated and presented as mean ± standard deviation. Data for each sample were collected from triplicate wells for each assay point ($n = 3$) and the experiments were performed in triplicate ($n = 9$).

2.5 Alkaline phosphatase activity

ALP activity in cell lysates was determined by measuring the release of p-nitrophenol (PNP) from disodium *p*-nitrophenyl phosphate. MC3T3-E1 cells were plated at 2×10^4 cells/well on test scaffolds and controls in 24 well plates. On day 3, corresponding to the time that cells reached confluence on cover slips, cells were cultured in α-MEM containing 10 mM β-glycerophosphate (Sigma®) and 50 μg/ml of ascorbic acid (Sigma®) to induce osteogenic differentiation [36, 37]. The osteogenic differentiation medium was changed every 2–3 days. On days 4, 6, 10, 14, 18, 22, and 26, cells were lysed by adding lysis buffer for 15 min. Lysis buffer was prepared by mixing phenylmethyl-sulfonyl fluoride (Sigma®) and CelLytic M (Sigma®). An aliquot of cell lysate was collected, centrifuged at 14,000 × *g* for 15 min at 4°C and stored at −80°C. ALP activities were expressed in nanomoles PNP per mg of protein per minute (nmol PNP/mg protein/min). For the ALP assay, absorbance was measured by spectrophotometry at 405 nm and calculated from a standard curve prepared using the PNP reagent (Sigma®) [38]. For the protein assay, absorbance was measured by spectrophotometry at 595 nm and protein concentrations of each sample were calculated from a standard curve prepared using bovine serum albumin (Sigma®) [39]. Data for each sample were collected from triplicate wells for each assay point ($n = 3$) and the experiments were performed in triplicate ($n = 9$).

2.6 Cell morphology and mineralized nodule formation

MC3T3-E1 cells were plated at 2×10^4 cells/well on test scaffolds and controls in 24 well plates. On day 3, when cells reached confluence on cover slips, cells were cultured in α-MEM containing 10 mM β-glycerophosphate and 50 μg/ml of ascorbic acid to induce osteogenic differentiation [36, 37]. The osteogenic differentiation medium was changed every 2–3 days. Cell morphology and mineralized nodule formation were checked routinely by phase contrast microscopy and examined by SEM on days 4, 10, and 18. The samples were fixed in 2.5% glutaraldehyde (Electron Microscopy Sciences, Washington, USA), 4% osmium tetroxide (Electron Microscopy Sciences), and dehydrated in a graded ethanol series to 100% ethanol. The samples were dried using a critical point dryer (Hitachi HCP-2,

Hitachi Science System Ltd., Japan) and sputter coated with platinum–palladium for SEM at 500× magnification. The presence of mineralized nodules was determined by staining with alizarin red-S (Sigma®) to identify calcium. The specimens were washed with PBS and fixed with ice-cold methanol for 10 min. The dye solution was then added in each well for 2–3 min. Data for each sample were collected from triplicate wells for each assay point ($n = 3$) and the experiments were performed in triplicate ($n = 9$).

2.7 Data collection and statistical analysis

Cell morphology and mineralized nodule formation data were analyzed by descriptive analysis. Scaffolding characteristics, cell attachment, cell proliferation, and ALP activity data were analyzed using SPSS for Windows Version 11.5. Data distribution was verified by the Komogorov–Smirnov Test. After testing the homogeneity of the variance, the Mann–Whitney Test was used to compare differences between groups. Statistical significance was set at $P < 0.05$.

3 Results

3.1 Scaffold characterization

SEM images revealed that all lyophilized test scaffolds had porous surfaces (Fig. 2). There were no statistically significant differences in the percentages of pores of each size (micro-, medium-sized, and macro-) present in the various test scaffolds (Table 1). All test scaffolds had a higher percentage in micropores than medium-sized pores or macropores. Statistically significant differences in area fractions were found among chitosan–collagen scaffolds (Table 1).

3.2 Cell attachment and cell proliferation

There were no statistically significant differences in cell attachment between control and test scaffolds at 5 and 24 h after cell attachment (Fig. 3a, b). MC3T3-E1 cells attached equally well to the control and test scaffolds, regardless of the DD and MW of the chitosan within the scaffolds.

MC3T3-E1 cells proliferated on both the control and the test scaffolds after cell attachment (Fig. 3c–g). When comparing the different DDs of chitosan with the same molecular weight, the OD values from the MTT assay for 50LMW-C were significantly higher than those of 80LMW-C on days 3, 5, 7, 10, and 14 (Fig. 3c–g), while the OD values from the MTT assay for 50HMW-C were significantly higher than those of 80HMW-C on days 5, 7, 10, and 14 (Fig. 3e–g). When comparing the different MW chitosan with the same DDs, the OD values from the MTT assay for 80HMW-C were significantly higher than those for 80LMW-C on day 5; on the contrary, the OD values for 50LMW-C were significantly higher than those for 50HMW-C on day 5 (Fig. 3d). As a result, the chitosan–

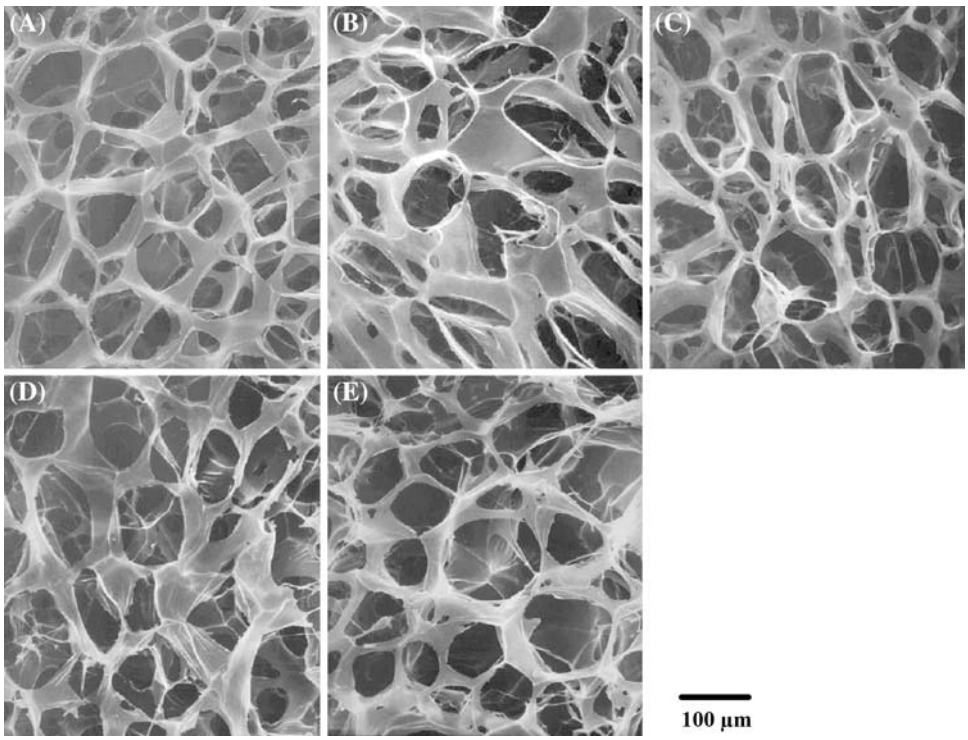

Fig. 2 Scanning electron microscopy images of collagen scaffolds and chitosan–collagen scaffolds. (**a**) Collagen scaffolds, (**b**) 80LMW-C, (**c**) 80HMW-C, (**d**) 50LMW-C, (**e**) 50HMW-C

Table 1 Chitosan–collagen scaffold characterization

Samples	*n*	% Pore size (mean ± SD)			Area fraction (mean ± SD)
		Micropore (0-19 μm)	Medium-sized pore (20-50 μm)	Macropore (51-100 μm)	
8OLMW-C	5	85 ± 2	13 ± 1	2 ± 2	66 ± 3
80HMW-C	5	84 ± 3	13 ± 1	3 ± 2	59 ± 2
5OLMW-C	5	85 ± 2	12 ± 1	3 ± 1	55 ± 2
50HMW-C	5	86 ± 1	12 ± 1	2 ± 1	62 ± 2

ImagePro Plus® Software Program version 3.0 for Windows was used to determine pore size and area fraction. Each value represented the mean ± SD of five samples. Statistical significance (*) was accepted at $P < 0.05$

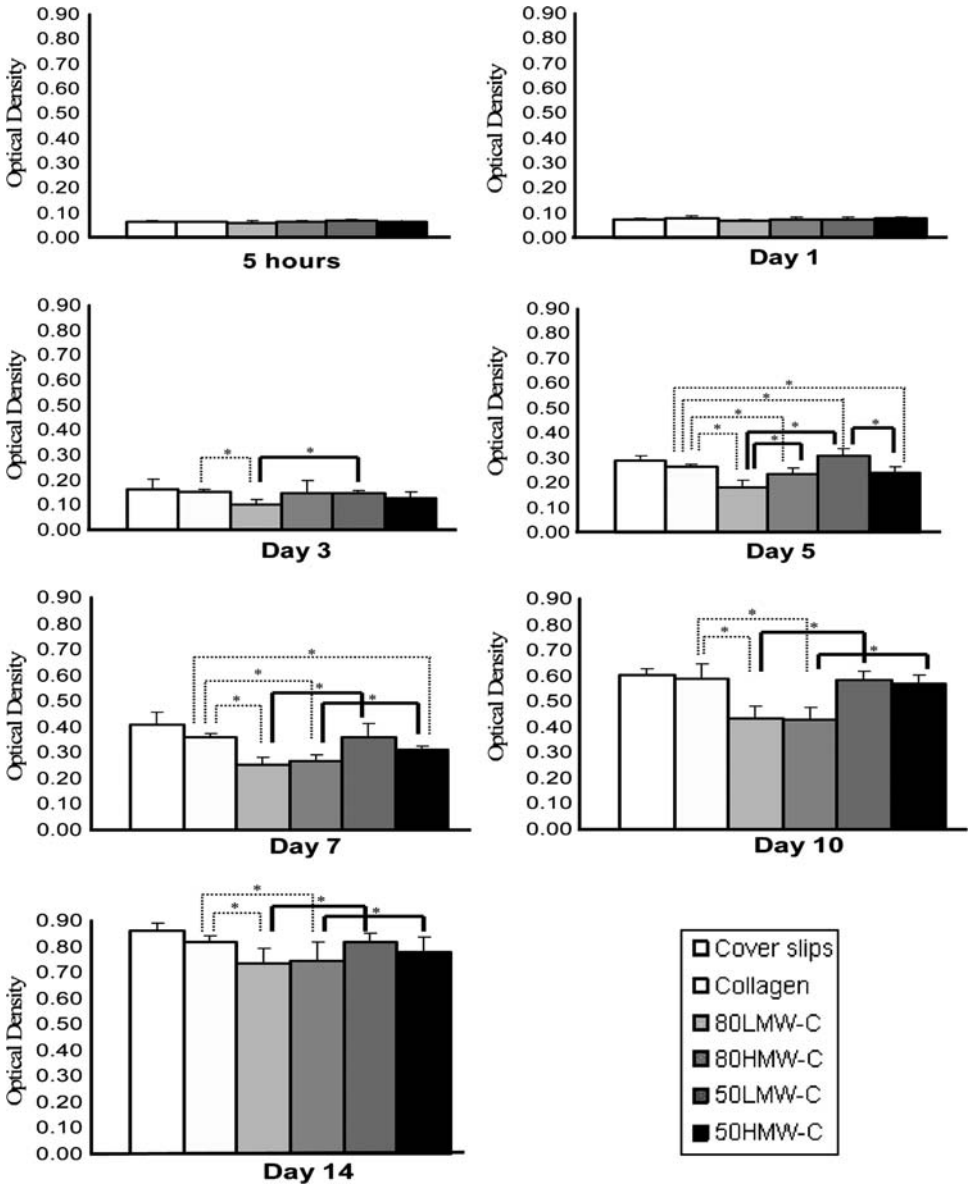

Fig. 3 Optical density readings of formazan formation at 5 h and on day 1 for cell attachment, and on days 3, 5, 7, 10, and 14 for cell proliferation. Each value represents the mean ± SD of nine samples. Statistical significance (*) was accepted at $P < 0.05$

collagen scaffolds that contained low-DD chitosan enhanced the proliferation of MC3T3-E1 cells as compared to chitosan–collagen scaffolds that contained high-DD chitosan, regardless of the MW of the chitosan.

3.3 Alkaline phosphatase activity

The ALP activity of MC3T3-E1 cells reached a maximum on day 4 after plating (first day after adding othe steogenic stimulus); thereafter, the ALP activity decreased gradually between days 6 and 10 and plateaued thereafter for cells cultured on both the controls and test scaffolds (Fig. 4a–g). These results suggest that all test and collagen scaffolds had similar patterns of ALP activity during differentiation.

In the early stage of differentiation, MC3T3-E1 cells on 50LMW-C and 50HMW-C had significantly greater ALP activity than did cells on 80LMW-C and 80HMW-C on days 4, 6, and 10 (Fig. 4a–c). These data indicate that the chitosan–collagen scaffolds that contained low-DD chitosan supported greater ALP activity in MC3T3-E1 cells than did chitosan–collagen scaffolds that contained high-DD chitosan, regardless of the MW.

3.4 Cell morphology and mineralized nodule formation

Figure 5 shows that MC3T3-E1 cells attached, spread and extended their cytoplasmic process (filopodia) on both controls and test scaffold surfaces and grew extensively on

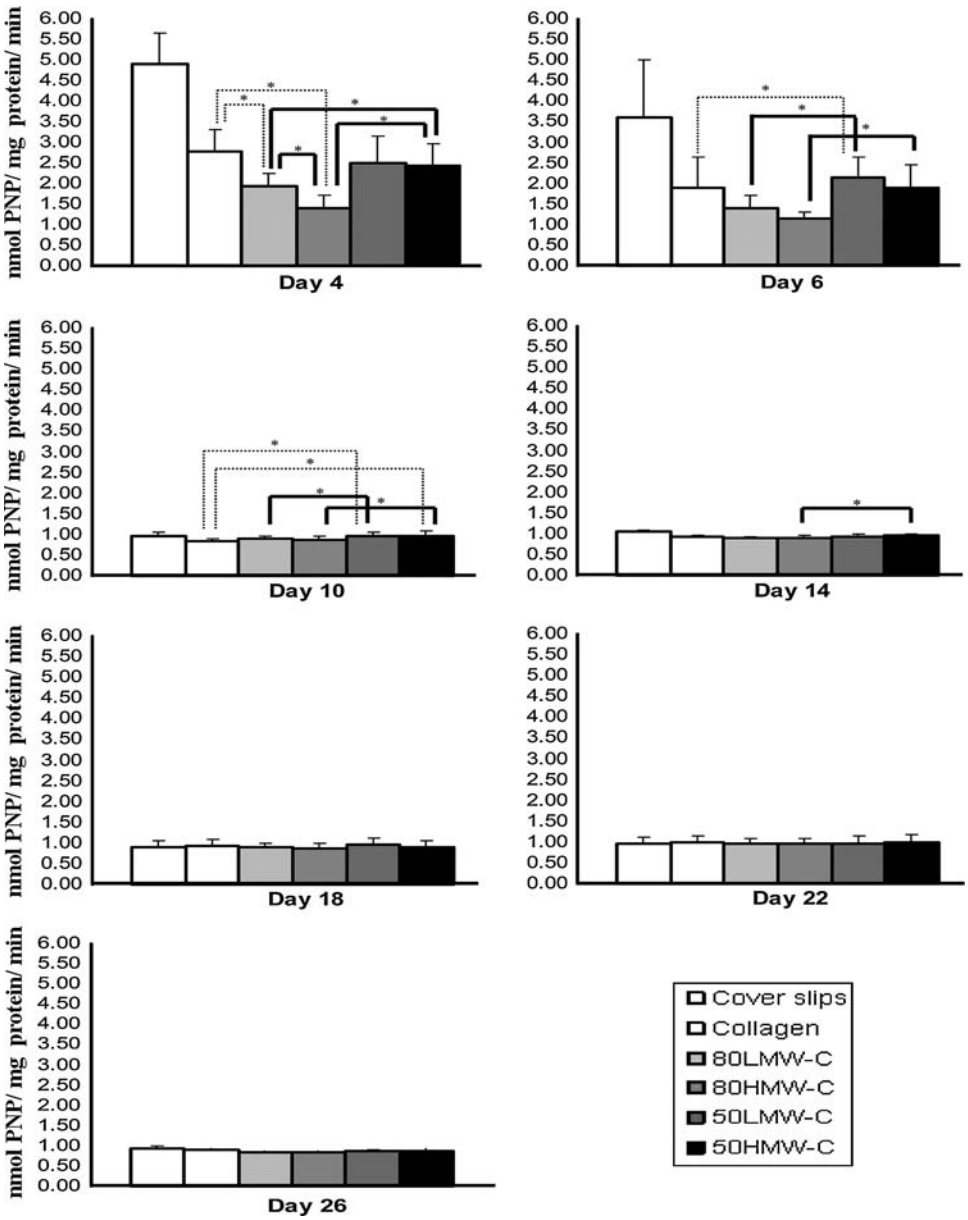

Fig. 4 Alkaline phosphatase activity of MC3T3-E1 cells on control and test scaffolds. ALP activity is expressed in nmol PNP/mg protein/min. Each value represents the mean ± SD of nine samples. Statistical significance (*) was accepted at $P < 0.05$

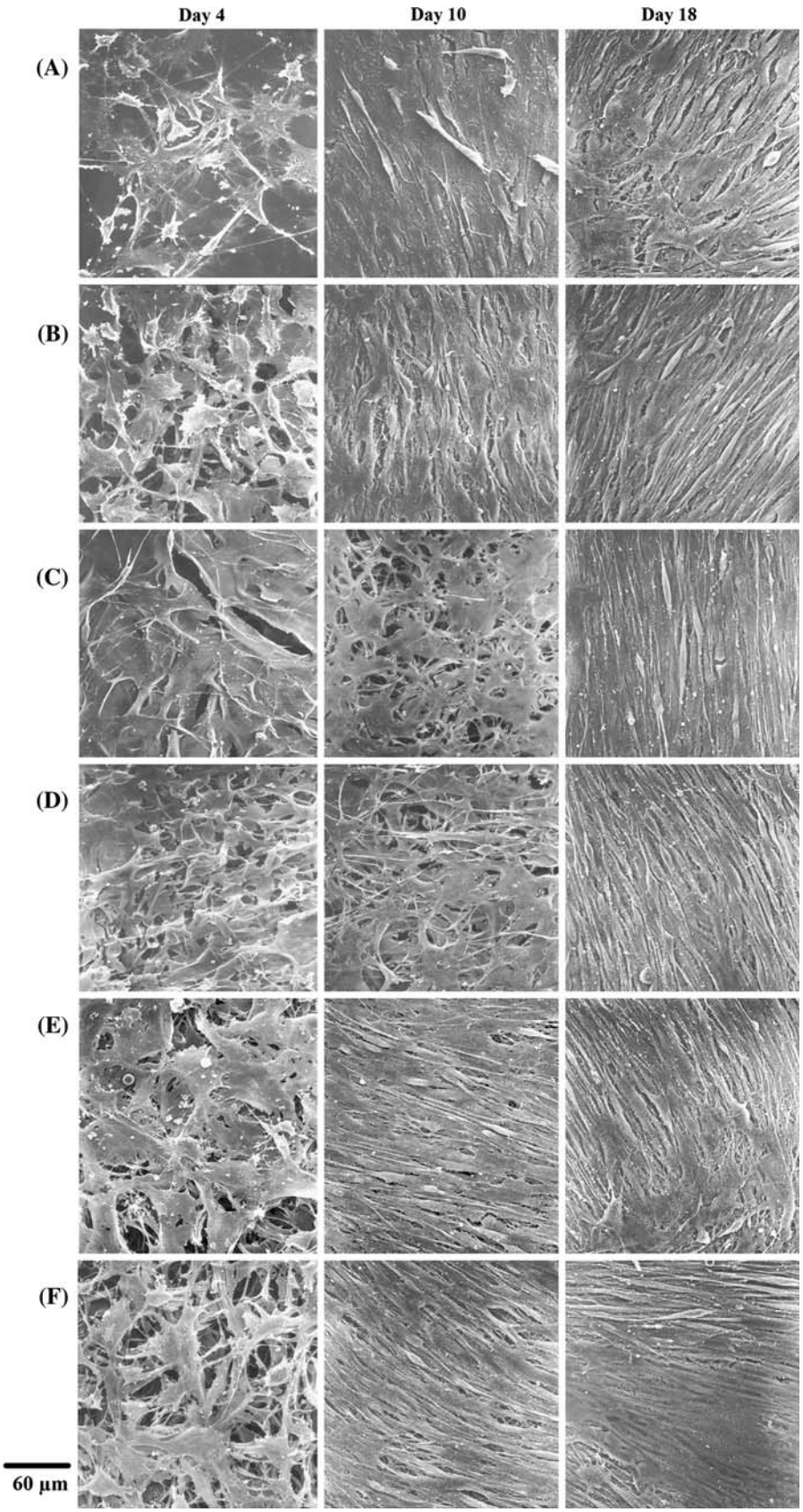

Fig. 5 Morphology of MC3T3-E1 cells on control and test scaffolds (500×). (**a**) Cover slips, (**b**) collagen, (**c**) 80LMW-C, (**d**) 80HMW-C, (**e**) 50LMW-C, (**f**) 50HMW-C

these scaffolds, although the growth rates varied. On day 4, the cover slips, collagen scaffolds and chitosan–collagen scaffolds with low-DD chitosan were covered with flatly-spread cells, more so than the chitosan–collagen scaffolds that contained high-DD chitosan. Nevertheless, the cells had not reached confluence; the bulk of the test scaffolds could be observed in the background. On day 10, MC3T3-E1 cells had grown into multilayers and intercellular connections were maintained through cytoplasmic elongations. Many anchoring processes were observed extending from cells to the biomaterial surface as well to the other cells. The controls and chitosan–collagen scaffolds with low-DD chitosan were fully covered by MC3T3-E1 cells; in contrast, the cell layers on the chitosan–collagen scaffolds with high-DD chitosan were not confluent. On day 18, the controls and all test scaffolds had multilayered cells and deposited matrix throughout the entire scaffolds. The mature MC3T3-E1 cells grew in parallel arrangement.

Mineralized nodule formation on test scaffolds and controls was confirmed by staining with alizarin red-S on day 22 of culture. The results showed that mineralized nodules were not present on collagen and chitosan–collagen scaffolds, but were present on the plain cover slips.

4 Discussion

Previous studies reported that chitosan–collagen composite materials showed potential for use in cell scaffolding for skin, cartilage and bone tissue engineering [40–42]. However, these studies used chitosans with only certain DDs or MWs in their investigations. In fact, the DD and the MW are fundamental determinants of all of the properties of chitosan and therefore directly affect the scaffold properties. As such, the DD and MW of the chitosan should be considered when chitosan–collagen scaffolds are evaluated for use in bone tissue engineering applications.

This study is the first to investigate the influence of the DD and MW of chitosan within chitosan–collagen scaffolds. In this initial test, we tested chitosans for which the ranges of DD and MW were quite broad. Because the range of DD for chitosans used in tissue engineering studies is so broad (varying from 40% to 98%) [10], we opted to test chitosans with extremely low (50%) and extremely high (80%) DDs in this study. Regarding the MWs of chitosans chosen for this study, we initially wanted to compare oligomers and polymers. However, pilot study indicated that oligomers could not form a scaffold and that the polymers would be a better choice. The MWs of chitosan polymers vary widely, ranging from 50 kDa to 2,000 kDa [10]; for this study we tested chitosans with MWs of 160 kDa and 1,000 kDa. In future investigations evaluating the use of chitosans for clinical applications it will important to select chitosans with the appropriate DD and MW for chitosan–collagen scaffolds.

Scaffolds used for tissue engineering must have a porous architecture to allow ingrowth of cells/tissues and transport of nutrients and waste products. The importance of pore size on tissue regeneration is emphasized by experiments demonstrating an optimum pore size of 5 μm for nutrient transportation and vascularization, greater than 20 μm for soft tissue ingrowth, 40–100 μm for osteoid ingrowth, and 100–350 μm for regeneration of bone [26, 43]. All of the lyophilized chitosan–collagen scaffolds tested in this study contained mostly micropores, but medium-sized pores and macropores were also present. There were no significant differences in the percentages of the different sized pores that were present among chitosan–collagen scaffolds (Table 1). However, there were statistically significant differences in area fraction among the different scaffolds (Table 1). These differences could have been the effect of the DD and MW of the chitosan within the chitosan–collagen scaffolds. From previous studies, the microstructures of chitosan scaffolds (such as porosity and interconnectivity) depended on the DD and MW of the chitosan [13, 28]. Other factors, (i.e., chitosan and/or collagen concentration, freezing temperature, and composition of chitosan with collagen) also played an important role in determining the microstructure of the scaffolds [26–28]; however, we controlled for these factors in this study.

Collagen is known to have excellent biocompatibility and osteoconductivity; however, its use in biological scaffolds is limited by its poor mechanical strength, fast degradation, and high cost. Chitosans are relatively inexpensive and have much greater mechanical strength than collagens; however, chitosans have lower bioactivity and greater brittleness. To improve the mechanical and biological properties of scaffolds, chitosan and collagen were combined [6, 44]. It was reported that chitosan–collagen sponges were porous, biocompatible, and able to the support growth and differentiation of osteoblasts to a greater extent than chitosan sponges [41, 45]; therefore, we evaluated the chitosan–collagen composite scaffolds in this study. It is possible that the presence of collagen confounded the effect of the chitosan in the chitosan–collagen scaffolds; the concentration of collagen (0.50% w/v) was the same in all test and collagen scaffolds, allowing us to detect differences between the collagen and chitosan–collagen scaffolds in this study.

No statistically significant differences in cell attachment were found among the test scaffolds and controls at 5 and 24 h (Fig. 3). MC3T3-E1 cells could attach equally well to the different chitosan–collagen scaffolds, regardless of the DD or MW of the chitosan. These findings are partially consistent with the results of Fakhry et al. [46] who found that MC3T3-E1 cells attach equally well to 0.25% and 1%

Chitosan-H (MW: 1,400,000; DD: 80%) and 0.5% Protasan (MW: 270,000; DD: 70%) 1 h after plating. On the contrary, Amaral et al. [20] reported that MG-63 cell attachment on chitosan films was dependent on the DA: a lower DA chitosan favored cell adhesion. Moreover, cell morphology can be regarded as an indicator of the affinity of the cells for a substratum. Flat cells are firmly attached by means of numerous attachment extensions and lamellopodia [47]. Figure 5 showed that MC3T3-E1 cell attached, spread and extended their cytoplasmic process on all test chitosan–collagen scaffolds. These findings indicate that chitosan–collagen scaffolds were biocompatible with MC3T3-E1 cells.

Cells plated on chitosan–collagen scaffolds that contained low-DD chitosan showed a significantly greater cell proliferation than cells plated on the scaffolds that contained high-DD chitosan. These data correspond to those from previous studies showing that the proliferation of any cell type was dependent on the DD of the chitosan in the substratum. According to Howling et al., chitosan with a relatively high-DD strongly stimulated human fibroblast proliferation while cells plated on chitosan with lower levels of deacetylation showed less activity. On the contrary, chitosan with a high-DD inhibited proliferation of human keratinocytes [17]. Seda et al. [48] reported that the higher deacetylated chitosan (>85%) scaffolds strongly supported fibroblastic cell proliferation as compared with less deacetylated chitosan (75–85%) scaffolds. In addition, Amaral et al. [20] reported that MG-63 cells grown on chitosan films with the lowest DA had a higher specific growth rate as compared to those grown on films with higher DA. The discrepancies in these results could be attributed to either the different cell types used in the experiments or the mechanism of cell adhesion to the chitosan surfaces. Different DDs result in different amounts of amine groups present at the surface. Cell adhesion to chitosan has been attributed to nonspecific electrostatic interactions between protonated amine groups and negatively charged carboxylate and sulfate groups found in cell surface proteoglycans [18, 49]; therefore cell-specific differences in the amounts and types of negatively charged surface molecules could result in cell-specific affinities for chitosans with different levels of deacetylation.

ALP, an early marker of osteoblast differentiation, is expressed at high levels near the end of the proliferative period and during the period of ECM deposition and is down-regulated after the mineralization stage [50, 51]. We found that as soon as the osteogenic stimuli were added to the culture medium, the ALP activity of the MC3T3-E1 cells on all test scaffolds increased sharply. Thereafter, ALP activity decreased gradually until day 10 of culture and then maintained at a constant level (Fig. 4). However, these findings disagree with those of Arpornmaeklong et al. [41] who reported that the ALP activity of MC3T3-E1 cells on 1:1 chitosan–collagen sponges was increased gradually and reached maximum on day 21 of culture. Possible reasons for this discrepancy include differences in scaffold thickness, cell density, concentration of organic phosphate, as well as the source of chitosan and collagen that were used. Moreover, ours is the first study to report that the DD of the chitosan within chitosan–collagen matrix influenced ALP activity of MC3T3-E1. Our data show that chitosan–collagen scaffolds that contain low-DD chitosan exhibit significantly more ALP activity than do scaffolds that contain high-DD chitosan.

Interestingly, only the plain cover slip controls allowed MC3T3-E1 cells to form mineralized nodules, whereas the test scaffolds did not. This might be due to the low level of ALP activity in the test scaffolds as compared to the plain cover slips, as shown in Fig. 4. If the ALP activity is too low, osteopontin expression will not be induced and the mineralized nodules will not form [51]. In addition, the chitosan–collagen and collagen scaffolds were three-dimensional while the plain cover slips were two-dimensional. Future experiments should address this issue whether the subculturing cell density, culture periods, or the concentration of osteogenic stimuli might influence mineralization. Moreover, much of the previous published data had been reported in the effect of the DD or MW of chitosan on flat surface such as membrane or coating; however, the present study showed that effect on porous materials.

Molecular weight is a crucial factor in determining the physicochemical properties of chitosan. Several publications have reported that the MW of chitosan influences its mechanical properties (tensile strength, modulus of elasticity, chain flexibility, etc.), chemical bonding, solubility, and degradability [12, 15, 26, 52]; in turn, these properties affect cell behavior. Nevertheless, our findings revealed no statistically significant differences in cell behavior between low and high-MW chitosan within chitosan–collagen scaffolds. As a result, it is possible that the MW of chitosan at 160 and 1,000 kDa had no effect on cell attachment and proliferation, ALP activity, or the ability to form mineralized nodules by MC3T3-E1 cells. However, results from an in vitro experimental model cannot recreate the complex interactions between cells and the ECM in vivo. Further studies using controlled in vivo models are needed in order to verify the results of this study.

5 Conclusion

MC3T3-E1 cells attach well on all chitosan–collagen scaffolds, but the proliferation and ALP activity of MC3T3-E1 cells depend on the DD of the chitosan contained in the scaffolds. On the contrary, the MW of the chitosan within

the chitosan–collagen scaffolds has no effect on MC3T3-E1 cells. Therefore, the DD of chitosan in chitosan–collagen scaffolds is a crucial factor in determining the biological behavior of MC3T3-E1 cells in vitro. The DD of the chitosan should be considered when using chitosan–collagen scaffolds in bone tissue engineering applications.

Acknowledgments This research was a part of a thesis to fulfill a requirement for a Master's program in Periodontics, Faculty of Dentistry, Mahidol University. The grant was supported by the Faculty of Graduate Studies, Mahidol University, Bangkok, Thailand.

References

1. I.V. Yannas, in *Scaffolding in tissue engineering*, ed. by P.X. Ma, J. Elisseeff (CRC Press, New York, 2006), p. 3
2. J.L.C. Susante, J. Pirper, P. Buma, T.H. Kuppevelt, H. Beuningen, P.M. Kraan et al., Biomaterials **22**, 2359 (2001)
3. S. Zhong, W.E. Teo, X. Zhu, R. Beuerman, S. Ramakrishna, L.Y. Yung, Biomacromolecules **6**, 2998 (2005). doi:10.1021/bm050318p
4. F.J. O'Brien, B.A. Harley, I.V. Yannas, L.J. Gibson, Biomaterials **26**, 433 (2005). doi:10.1016/j.biomaterials.2004.02.052
5. M.N.V. Ravie kumar, React. Funct. Polym. **43**, 1 (2000). doi:10.1016/S1381-5148(98)00082-0
6. W. Tan, R. Krishnaraj, T.A. Desai, Tissue Eng. **7**, 203 (2001). doi:10.1089/107632701300062831
7. M. Gingras, I. Paradis, F. Berthod, Biomaterials **24**, 1653 (2003). doi:10.1016/S0142-9612(02)00572-0
8. L. Ma, C. Gao, Z. Mao, J. Zhou, J. Shen, X. Hu et al., Biomaterials **24**, 4833 (2003). doi:10.1016/S0142-9612(03)00374-0
9. L. Peng, X.R. Cheng, J.W. Wang, D.X. Xu, G. Wang, J. Bioact. Compat. Polym. **21**, 207 (2006). doi:10.1177/0883911506065100
10. A. Gallardo, M. R. Aguilar, C. Elvira, C. Peniche, J. S. Roman, in *Biodegradable systems in tissue engineering and regenerative medicine*, ed. by R. Reis, J. S. Roman (CRC Press, Florida, 2004), p. 145
11. D. W. Hutmacher, K. W. Ng, H. L. Khor, in *Biodegradable systems in tissue engineering and regenerative medicine*, ed. By R. Reis, J. S. Roman (CRC Press, Florida, 2004), p. 509
12. A.D. Martino, M. Sittinger, M.V. Risbud, Biomaterials **26**, 5983 (2005). doi:10.1016/j.biomaterials.2005.03.016
13. C. Tangsadthakun, S. Kanokpanont, N. Sanchavanakit, R. Pichyangkura, T. Banaprasert, Y. Tabata et al., J. Biomater. Sci. Polym. Ed. **18**, 147 (2007). doi:10.1163/156856207779116694
14. Q.Z. Wang, X.G. Chen, N. Liu, S.X. Wang, C.S. Liu, X.H. Meng et al., Carbohydr. Polym. **65**, 194 (2006). doi:10.1016/j.carbpol.2006.01.001
15. R.H. Chen, H.D. Hwa, Carbohydr. Polym. **29**, 353 (1996). doi:10.1016/0144-8617(96)00005-7
16. M. Prasitsilp, R. Jenwithisuk, K. Kongsuwan, N. Damrongchai, P. Watts, J. Mater. Sci.: Mater. Med. **11**, 773 (2000). doi:10.1023/A:1008997311364
17. G.I. Howling, P.W. Dettmar, P.A. Goddard, F.C. Hampson, M. Dornish, E.J. Wood, Biomaterials **22**, 2959 (2001). doi:10.1016/S0142-9612(01)00042-4
18. C. Chatelet, O. Damour, A. Domard, Biomaterials **22**, 261 (2001). doi:10.1016/S0142-9612(00)00183-6
19. J.S. Mao, Y.L. Cui, X.H. Wang, Y. Sun, Y.J. Yin, H.M. Zhao et al., Biomaterials **25**, 3973 (2004). doi:10.1016/j.biomaterials.2003.10.080
20. I.F. Amaral, A.L. Cordeiro, P. Sampaio, M.A. Barbosa, J. Biomater. Sci. Polym. Ed. **18**, 469 (2007). doi:10.1163/156856207780425068
21. K.M. Varum, M.M. Myhr, R.J.N. Hjerde, O. Smidsrod, Carbohydr. Res. **299**, 99 (1997). doi:10.1016/S0008-6215(96)00332-1
22. K. Tomihata, Y. Ikada, Biomaterials **18**, 567 (1997). doi:10.1016/S0142-9612(96)00167-6
23. Y. Hidaka, M. Ito, K. Mori, H. Yagasaki, A.H. Kafrawy, J. Biomed. Mater. Res. **46**, 418 (1999). doi:10.1002/(SICI)1097-4636(19990905)46:3<418::AID-JBM15>3.0.CO;2-T
24. E.B. Denbas, M. Odabasi, J. Appl. Polym. Sci. **76**, 1637 (2000). doi:10.1002/(SICI)1097-4628(20000613)76:11<1637::AID-APP4>3.0.CO;2-Q
25. E.B. Denbas, E. Kilicay, C. Birlikseven, E. Ozturk, React. Funct. Polym. **50**, 225 (2002). doi:10.1016/S1381-5148(01)00115-8
26. S.V. Madihally, H.W.T. Matthew, Biomaterials **20**, 1133 (1999). doi:10.1016/S0142-9612(99)00011-3
27. W.W. Thein-Han, Y. Kittiyanant, J. Biomed. Mater. Res. Part B Appl. Biomater. **80B**, 92 (2007). doi:10.1002/jbm.b.30573
28. D.L. Nettles, S.H. Elder, J.A. Gilbert, Tissue Eng. **8**, 1009 (2002). doi:10.1089/107632702320934100
29. M. Ahmad, M. McCarthy, G. Gronowicz, Biomaterials **20**, 211 (1999). doi:10.1016/S0142-9612(98)00152-5
30. D. Wang, K. Christensen, K. Chawla, G. Xiao, P.H. Krebsbach, R.T. Franceschi, J. Bone Miner. Res. **14**, 893 (1999). doi:10.1359/jbmr.1999.14.6.893
31. C. V. Gay, H. J. Donahue, C. A. Siedlecki, E. Vogler, in *Bone tissue engineering*, ed. by J. O. Hollinger, T. A. Einhorn, B. A. Doll, C. Sfeir (CRC Press, Florida, 2005), p. 43
32. R. L. Whistler, in *Industrial gums: Polysaccharides and their derivatives*, ed. by R. L. Whistler, J. N. BeMiller (Academic Press, California, 1993), p. 601
33. R.A.A. Muzzarelli, R. Rocchetti, Carbohydr. Polym. **5**, 461 (1985). doi:10.1016/0144-8617(85)90005-0
34. R. O'Leary, E.J. Wood, In Vitro Cell Dev. Biol. **39**, 204 (2003). doi:10.1290/1543-706X(2003)039<0204:ANIVDW>2.0.CO;2
35. T. Mosmann, J. Immunol. Methods **65**, 55 (1983). doi:10.1016/0022-1759(83)90303-4
36. M.J. Coelho, A.T. Cabral, M.H. Fernandes, Biomaterials **21**, 1087 (2000). doi:10.1016/S0142-9612(99)00284-7
37. M.J. Coelho, M.H. Fernandes, Biomaterials **21**, 1095 (2000). doi:10.1016/S0142-9612(99)00192-1
38. L. Marinucci, C. Lilli, T. Baroni, E. Becchetti, S. Belcastro, C. Balducci, P. Locci, J. Periodontol. **72**, 753 (2001)
39. M.M. Bradford, Anal. Biochem. **72**, 248 (1976). doi:10.1016/0003-2697(76)90527-3
40. F.M. Braye, A. Stefani, E. Venet, D. Pieptu, E. Tissot, O. Damour, Br. J. Plast. Surg. **54**, 532 (2001). doi:10.1054/bjps.2001.3620
41. P. Arpornmaeklong, N. Suwatwirote, P. Pripatanont, K. Oungbho, Int. J. Oral Maxillofac. Surg. **36**, 328 (2007). doi:10.1016/j.ijom.2006.09.023
42. J.E. Lee, K.E. Kim, I.C. Kwon, H.J. Ahn, S.H. Lee, H. Cho et al., Biomaterials **25**, 4163 (2004). doi:10.1016/j.biomaterials.2003.10.057
43. S. Yang, K.-F. Leong, Z. Du, C.-K. Chua, Tissue Eng. **7**, 679 (2001). doi:10.1089/107632701753337645
44. M.N. Taravel, A. Domard, Biomaterials **17**, 451 (1996). doi:10.1016/0142-9612(96)89663-3
45. P. Arpornmaeklong, P. Pripatanont, N. Suwatwirote, Int. J. Oral Maxillofac. Surg. **37**, 357 (2008). doi:10.1016/j.ijom.2007.11.014
46. A. Fakhry, G.B. Schneider, R. Zaharias, S. Senel, Biomaterials **25**, 2075 (2004). doi:10.1016/j.biomaterials.2003.08.068
47. D.J. Trylovich, C.M. Cobb, D.J. Pippin, P. Spencer, W.J. Killoy, J. Periodontol. **63**, 1992 (1992)

48. T.R. Seda, A. Karakecili, M. Gumusderelioglu, J. Mater. Sci.: Mater. Med. **18**, 1665 (2007). doi:10.1007/s10856-007-3066-x
49. I. Henriksen, K.L. Green, J.D. Smart, G. Smistad, J. Karlsen, Int. J. Pharm. **145**, 231 (1996). doi:10.1016/S0378-5173(96)04776-X
50. G.R. Beck, E.C. Sullivan, E. Moran, B. Zerler, J. Cell. Biochem. **68**, 269 (1998). doi:10.1002/(SICI)1097-4644(19980201)68:2<269::AID-JCB13>3.0.CO;2-A
51. G.R. Beck, B. Zerler, E. Moran, Proc. Natl. Acad. Sci. USA **97**, 8352 (2000). doi:10.1073/pnas.140021997
52. Y. Yin, F. Ye, J. Cui, F. Zhang, X. Li, K. Yao, J. Biomed. Mater. Res. **67A**, 844 (2003). doi:10.1002/jbm.a.10153